

SOLVING THE ORIENTATION-DUALITY PROBLEM FOR A CIRCULAR FEATURE IN MOTION

D. He and B. Benhabib*

Computer Integrated Manufacturing Laboratory (CIMLab), Department of Mechanical
and Industrial Engineering

University of Toronto, 5 King's College Road, Toronto, Ontario, M5S 3E8,

*email:beno@mie.utoronto.ca

Abstract

Circular features have been commonly used in numerous computer vision application areas for 3-D pose estimation. However, the estimation of such a feature's pose from 2-D image coordinates results in an orientation-duality problem. Namely, although the 3-D position of the circle's center can be uniquely identified, the solution process yields two different feasible orientations, of which only one is the true solution. This duality problem is normally addressed through the acquisition of a second image in the case of a "static" feature. This solution, however, would not be applicable to "features in motion".

In this paper, several methods are presented for the solution of the orientation-duality problem for circular features that are in motion. The first approach is applicable to those features moving on a 3-D line with constant orientation or to those which are moving on a plane with general motion. The second approach relies on the existence of additional object features, such as points or lines, which are co-planar to the circular

feature. In this case, the circular feature can undergo an arbitrary 3-D motion. Experimental results verify the validity of the proposed methods.

1. Introduction

Motion study from consecutive images is one of the key issues in the development of a vision system for moving-object recognition. There exist two common approaches: Feature-based methods and optical-flow methods. Feature-based techniques require that correspondence be established between a sparse set of features extracted from one image with those extracted from the next image in the sequence. Many features have been used to establish correspondence, including points, lines, planes, conics and combination of these features, [28-33T]. Although numerous techniques have been established for extracting and establishing feature correspondence, they are normally suitable for simple situations (i.e., non-general motions), [12T].

An image sequence of a single point or a line segment may not be sufficient for estimating all the necessary 3-D motion parameters. Therefore, a more compact primitive would be better suited for this problem. In this context, conics, particularly circles, provide the most important clues to 3-D interpretation of images next to straight lines for the following reasons, [13]:

1. The conic is a more compact primitive than points and line segments, and it contains the pose information of a rigid-body object;
2. The representation of a conic is a symmetric matrix, which is easy to manipulate mathematically;
3. Circles have shown to have the important property of high image-location accuracy; and,
4. For motion analysis, no point-wise correspondence between two circles are necessary.

In general, motion and structure parameters cannot be estimated from only two images of a single conic [13]. Two images of at least three conics are needed in order to solve the complex non-linear problem.

The active-vision system developed in our laboratory, for the recognition of moving objects, uses (artificial) circular features as targets to be tracked, where correspondence between at least two consecutive images provides a unique solution to the 3-D pose-estimation problem. As mentioned above, however, for a circle, with a known radius, a closed-form solution exists for determining its 3-D static pose from a single image, with the exception of having two possible orientations. A second image of the static circle is then acquired to determine the true orientation based on the circle's eccentricity change. This suggests that, in general, for a circular feature of known size, two images may be sufficient to uniquely determine its 3-D general-motion parameters. No previous work, addressing this issue, has been reported in the literature.

In this paper, Section 2 will first briefly review the closed-form solution method presented in [12] for the circular feature pose-estimation problem. Subsequently, Section 3 will introduce the orientation-duality problem. Sections 4 and 5 will propose techniques to solve this problem using motion constraints and additional features, respectively.

2. Pose Estimation of Circular Features

There have been several active-vision systems proposed in the literature for recognizing objects in motion [1-7]. However, recognition techniques used by these systems are highly computationally intensive and sensitive to noise. Object pre-conditioning has been proposed in numerous occasions to help (static-) object recognition systems in this regard [8,9]. For the 3-D pose estimation of circular features, for example, several approximate and exact solution methods have been proposed [10-12]. The present paper is a follow-up to our own work on static-object recognition earlier reported in [12]. Thus, as abovementioned, our current objective is "*the use of circular features (i.e., markers) in the recognition of moving objects.*"

Circular features undergo perspective projection and would be perceived as elliptical shapes in arbitrarily acquired images. Estimation of the five elliptical parameters of this image is the first step toward the determination of the 3-D pose of the circular

feature. These parameters can be obtained by using a least-squares type fitting technique, [38T].

The pose of a circular feature can be solved for analytically, [12]. First, based on the elliptical parameters of its image, the 3-D orientation is estimated; subsequently, based on the estimated orientation, the 3-D position of the feature is calculated.

Circular-feature pose estimation is equivalent to the solution of the following problem: Given a 3-D conic surface, defined by a base (the perspective projection of a circular feature in the image plane) and a vertex (the center of the camera's lens) with respect to a reference frame, determine the pose of the plane (with respect to the same reference frame), which intersects the cone and generates a circular curve, Figure 1, [12].

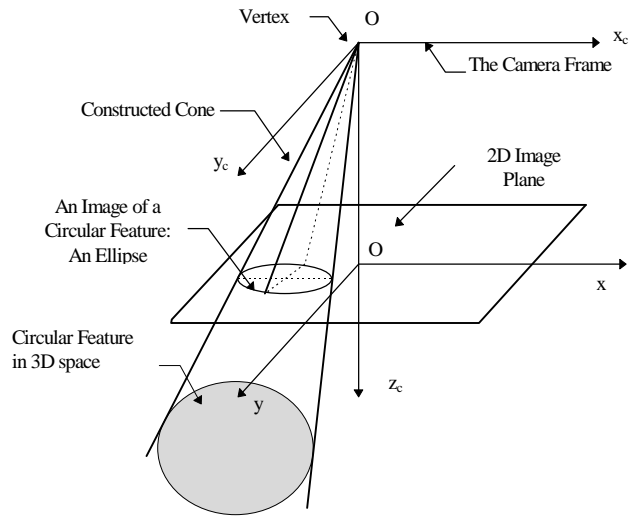


Figure 1. Circular-feature pose estimation [12].

The general form of the equation of a cone with respect to the image frame is as follows:

$$\begin{aligned}
 & ax^2 + by^2 + cz^2 + 2fyx + 2gzx \\
 & + 2hxy + 2ux + 2vy + 2wz + d = 0.
 \end{aligned} \tag{1}$$

An intersection plane can be defined by $lx + my + nz = 0$. Therefore, the problem of finding the coefficients of the equation of a plane, for which the intersection is circular, can be expressed mathematically as: determine l , m and n such that the intersection of the conical surface with the following surface is a circle: $lx + my + nz = 0$, where $l^2 + m^2 + n^2 = 1$.

The above 3-D-orientation problem can be solved analytically by considering the equation of a cone in its central form, [4T]. Thus, it is required to find the coefficients of the equation of a particular plane (with respect to the canonical XYZ -frame),

$$l X + m Y + n Z = p, \quad (2)$$

whose intersection with a central cone,

$$\lambda_1 X^2 + \lambda_2 Y^2 + \lambda_3 Z^2 = 0, \quad (3)$$

would be a circle.

Three possible cases exist:

Case I: If $\lambda_1 < \lambda_2$, there exist four solutions to the problem. However, these are four symmetrical solutions with respect to the origin of the XYZ -frame and, consequently, represent only two unique solutions. If one takes the solutions on the positive section of Z -axis, then, the two solutions would be:

$$\begin{cases} n = +\sqrt{\frac{\lambda_1 - \lambda_3}{\lambda_2 - \lambda_3}} \\ m = \pm\sqrt{\frac{\lambda_2 - \lambda_1}{\lambda_2 - \lambda_3}} \\ l = 0. \end{cases} \quad (4)$$

Case II: If $\lambda_1 > \lambda_2$, following the same arguments for Case I, two solutions can be derived, which would be acceptable only if $\lambda_1 > \lambda_2$:

$$\begin{cases} n = +\sqrt{\frac{\lambda_2 - \lambda_3}{\lambda_1 - \lambda_3}} \\ m = 0 \\ l = \pm\sqrt{\frac{\lambda_1 - \lambda_2}{\lambda_1 - \lambda_3}}. \end{cases} \quad (5)$$

Case III: If $\lambda_1 = \lambda_2$, the equation of the central cone represents a right circular cone, (which implies that the central surface normal of the circular feature passes through the origin of the camera frame), and thus, intersection between any plane in the form $Z = k$ and the cone will generate a circular curve. Thus, there exists only one solution:

$$\begin{cases} n = 1 \\ m = 0 \\ l = 0. \end{cases} \quad (6)$$

It can be concluded that there exist two possible orientations. To obtain a unique acceptable solution, an extra geometrical constraint, such as the change of eccentricity in a second image, has to be obtained.

To solve for a unique solution for a marker's position, the radius of the circular feature has to be known. There exist two solutions: one on the positive Z -axis, and one the negative Z -axis, [12]. Only the positive one is acceptable in our case (being located in front of the camera).

3. Solutions to the Orientation Duality Problem for Circular Features in Motion

The eccentricity of a circular feature's image acquired by a camera, whose focal axis is perfectly aligned with the circle's normal should be equal to one. Therefore, the

change of eccentricity of the ellipse in the second image, acquired after a known movement of the camera, would yield the true orientation of the circular feature. This simple technique, however, can only be applied to static features.

For circular features in motion, several new effective techniques will be presented below to distinguish the true orientation from the false one via the use of consecutive images. In general, if a circular feature undergoes arbitrary 3-D motion, it is impossible to find its true orientation directly, since both orientations found at a specific position could be true under certain spatial transformation. In other words, without additional information, the true orientation of the feature cannot be determined from consecutive images. Two types of information are used herein to address this problem. One approach is to constrain the object motion, e.g., to consider only pure 3-D translation or planar motion. Another approach is to consider extra co-planar features, other than the viewed circular-feature, such as points and lines, to provide structural information about the object.

3.1 Pure 3-D Translation

By definition, an object is under (pure) translation in 3-D when no rotational motion exists about any axis. Therefore, when a circle is translating, the true solution of the circle's surface normal can be found directly from two consecutive images: *The true surface normal is the one that remains constant in both images.*

Figure 2 depicts a circle moving from Position 1 to Position 2. At Position 1, we obtain two possible unit surface-normal vectors of the circle, \mathbf{n}_1 and \mathbf{n}_2 . Likewise, we obtain \mathbf{n}_1 and \mathbf{n}_2 for the second image acquired at Position 2. Let ω and ω define the unit directional vectors pointing from the circular-feature's center to the camera's focal point, which pass through the centers of the images ellipses. If \mathbf{n}_1 is assumed to represent

the true orientation, it would remain constant¹ during the translation. Based on the symmetry of the two possible orientations with respect to ω , change of ω would then necessarily imply change in n_2 .

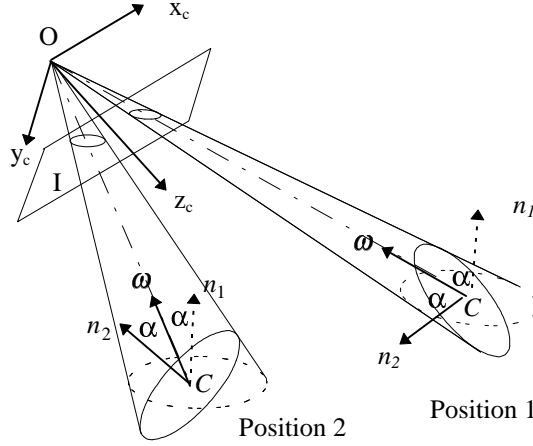


Figure 2. Circular feature in translational motion.

The false orientation of a circular feature changes, except when the circular marker is translating along a straight line toward the camera's focal center, i.e., when $\omega = \omega$. Let the axial unit vector ω be defined herein as follows,

$$\begin{aligned}\omega &= \frac{I}{\sqrt{(k_1 + k_2)^2 + (l_1 + l_2)^2 + (m_1 + m_2)^2}} [(k_1 + k_2) \cdot i + (l_1 + l_2) \cdot j + (m_1 + m_2) \cdot k] \\ &= -\frac{I}{\sqrt{x_c^2 + y_c^2 + z_c^2}} (x_c \cdot i + y_c \cdot j + z_c \cdot k),\end{aligned}\quad (7)$$

¹ Herein and in the following sections the use of empirically defined thresholds is proposed for determining tangible changes in orientation vectors between consecutive images.

where (x_c, y_c, z_c) represent Point C, (k_1, l_1, m_1) and (k_2, l_2, m_2) are the components of the orientation vectors \mathbf{n}_1 and \mathbf{n}_2 , respectively, and \mathbf{i}, \mathbf{j} and \mathbf{k} are unit vectors, all defined with respect to the camera frame, Figure 1.

Equation (7) can also be expressed in its component form as,

$$\omega_x = k_1 + k_2 = -\sqrt{\frac{r^2}{x_c^2 + y_c^2 + z_c^2}} \cdot x_c, \quad (8-a)$$

$$\omega_y = l_1 + l_2 = -\sqrt{\frac{r^2}{x_c^2 + y_c^2 + z_c^2}} \cdot y_c, \quad (8-b)$$

$$\omega_z = m_1 + m_2 = -\sqrt{\frac{r^2}{x_c^2 + y_c^2 + z_c^2}} \cdot z_c, \quad (8-c)$$

where r is defined as

$$r^2 = (k_1 + k_2)^2 + (l_1 + l_2)^2 + (m_1 + m_2)^2,$$

and represents the magnitude of ω .

Similarly, for the second image, the vector ω is defined as

$$\omega_x = k_1 + k_2 = -\sqrt{\frac{r^2}{x_c^2 + y_c^2 + z_c^2}} \cdot x_c, \quad (9-a)$$

$$\omega_y = l_1 + l_2 = -\sqrt{\frac{r^2}{x_c^2 + y_c^2 + z_c^2}} \cdot y_c, \quad (9-b)$$

$$\omega_z = m_1 + m_2 = -\sqrt{\frac{r^2}{x_c^2 + y_c^2 + z_c^2}} \cdot z_c. \quad (9-c)$$

Ill-Conditioned Case:

When $\mathbf{n}_1=\mathbf{n}_1$ and $\mathbf{n}_2=\mathbf{n}_2$, in two consecutive images, the duality problem cannot be solved by the proposed technique. Then, by definition of ω and ω , we have

$$\omega = \omega. \quad (10)$$

Conjecture 1: Equation (10) indicates that the problem is ill-conditioned when the object (purely) translates along the line OC.

Experiments:

Experimental Set-up: The imaging system used for all the experiments repeated herein comprised a JVC CCD color camera, with a 640x480 resolution, mounted on a six degree-of-freedom GMF S100 robot's end effector. A PC-based PIP Matrox digitizer board with a 640x480 resolution was utilized for the acquisition of object images. The camera was equipped with a 25 mm lens and normally placed 500 mm away from the circular features. The camera's extrinsic and intrinsic parameters were obtained using the mono-view, non-co-planar point technique proposed in [59T]. Additional direct measurements were made to relate the camera's frame to the robot's base frame. Measurement errors in both x and y directions were less than 0.5%.

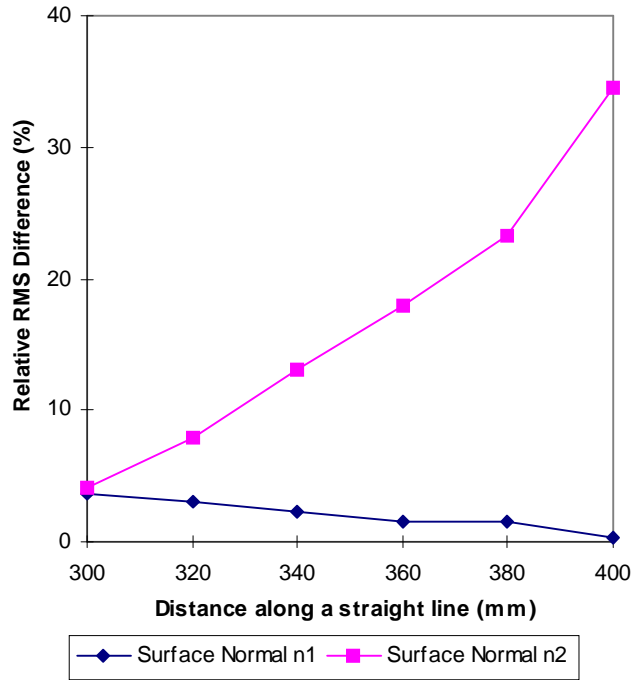
One must note that the selection of the camera's nominal distance to a circular feature is dependent on the feature's size. Also, the orientation of the camera must be chosen to maximize visibility of the feature. Both these issues were addressed in our earlier studies, [35T, 38T], and the results implemented in this current work.

Experimental Procedure: Experiments were conducted to verify Conjecture 1 stated above. For increased accuracy, the mobile camera was translated along a certain 3-D path to simulate (feature's) translational motion, while the object itself was kept stationary. At several positions along the path, the possible surface normals of the circular marker on the object, \mathbf{n}_1 and \mathbf{n}_2 , were estimated. The relative Root-Mean-Square (RMS) differences

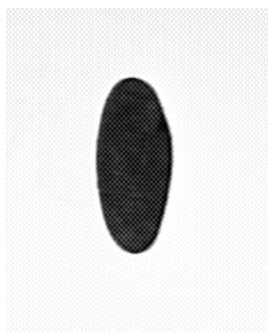
between the vectors and their initial values, i.e., $\frac{\|\mathbf{n}_1 - \mathbf{n}_1\|}{\|\mathbf{n}_1\|}$ and $\frac{\|\mathbf{n}_2 - \mathbf{n}_2\|}{\|\mathbf{n}_2\|}$, were calculated

and recorded.

In the first test, the object pseudo-translated along a straight line that does not coincide with ω . The intervals between consecutive test positions were set at approximately 20 mm. At every instant, the RMS difference was calculated with respect to the original normals. As shown in Figure 3, the relative RMS differences in \mathbf{n}_2 are significantly greater than those in \mathbf{n}_1 . The RMS-reduction trend of \mathbf{n}_1 in Figure 3 is coincidental and primarily due to favorable alignment of the camera's optical axis with respect to the normal of the circular feature.

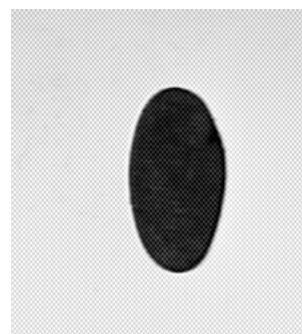


(a)



(i)

(ii)



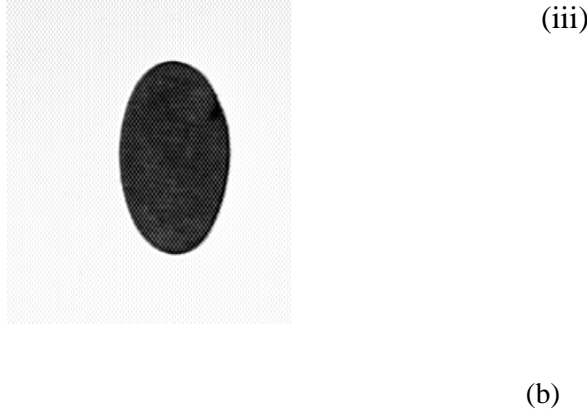


Figure 3. Translation along the straight line: (a) Experimental results; and, (b) Three consecutive images.

The expected ill-conditioned case was simulated by translating the camera away from the object along the vector ω . Measurements were taken at 40 mm intervals. The RMS differences for this case, for both n_1 and n_2 are shown in Figure 4. The results clearly show that both n_1 and n_2 remain relatively constant, and therefore the duality problem remains unsolved.

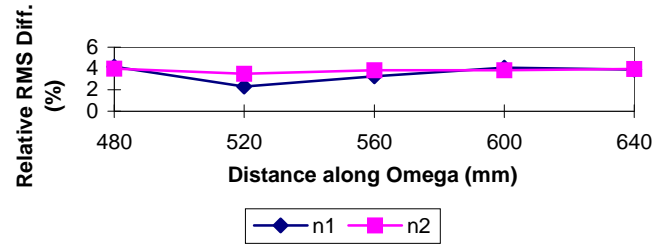


Figure 4. Translation along ω .

3.2 General Planar motion

When a circular feature moves in a general planar motion, it has three degrees of freedom, (x, y, θ) . Figure 5 depicts a surface normal n , which is translated from its initial

position (x_c, y_c, z_c) to a new position (x_c, y_c, z_c) . It is rotated concurrently about the z axis by $\Delta\theta$. Namely, the vector \mathbf{n} is transformed into \mathbf{n}' .

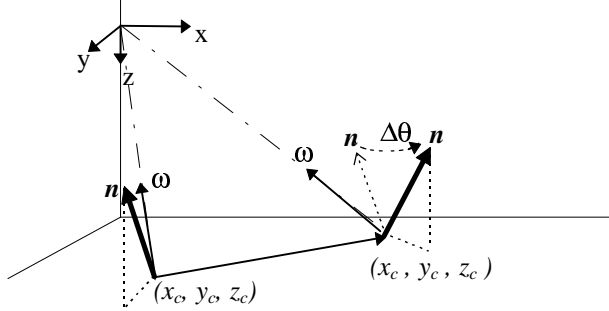


Figure 5. Planar motion of the normal of a circular feature.

Since the motion is planar, the z component of the vector \mathbf{n} will remain constant.

Conjecture 2: *The z component of the false orientation vector changes, while that of the true orientation remains the same, with the exception of certain ill-conditioned cases.*

Figure 6 depicts Conjecture 2, stated above, where only a rotation about the z axis is considered. When the true surface normal \mathbf{n}_1 rotates around the z axis, the false solution \mathbf{n}_2 rotates correspondingly, so as to maintain the symmetry with respect to ω . Both vectors \mathbf{n}_1 and \mathbf{n}_2 generate respective circular paths, P_1 and P_2 . P_1 lies in a plane parallel to the feature-motion plane because only rotation about the z axis is permitted. Since ω is an arbitrary vector, P_2 would normally lie in a plane that is not parallel to the feature-motion plane. Thus, a rotation of \mathbf{n}_1 and corresponding rotation of \mathbf{n}_2 would result in the change of the z component of \mathbf{n}_2 .

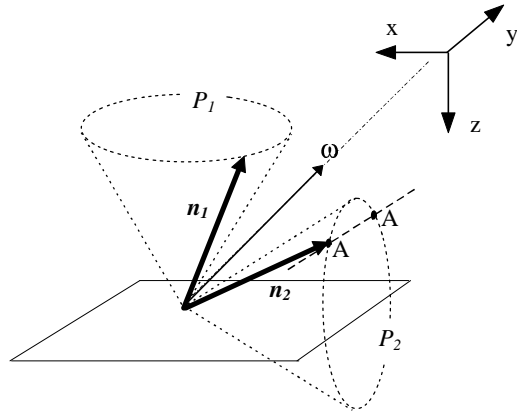


Figure 6. Changes in the z component of \mathbf{n}_2 .

The problem becomes ill-conditioned, when \mathbf{n}_2 maintains the same z component for a specific motion of \mathbf{n}_1 . For every motion, there only exist two such possible positions on P_2 , A and A'.

In light of this reasoning, the procedure for solving the orientation-duality problem for a circular feature moving in planar motion can be summarized as follows:

Step 1: Acquire the first image of the circular feature, and calculate: (i) its center (x_c, y_c, z_c) , and (ii) the two possible orientation vectors \mathbf{n}_1 and \mathbf{n}_2 .

Step 2: Check if the z components of both \mathbf{n}_1 and \mathbf{n}_2 are equal. If they are, i.e., $m_1=m_2$, the proposed technique cannot be used, since \mathbf{n}_1 and \mathbf{n}_2 cannot be distinguished by their z components. We return to Step 1 to acquire a new image different than the first.

Otherwise, i.e., $m_1 \neq m_2$, we proceed to Step 3.

Step 3: Acquire a second image of the same feature in motion (after a period of time), and, as in Step 1, calculate (i) its center (x_c, y_c, z_c) , and (ii) the two possible orientation vectors \mathbf{n}_1 and \mathbf{n}_2 .

Step 4: Compare the z components of the orientation vectors. If one of the z components remains constant between the two images, i.e., $m_1=m_1$, while the other one

changes, i.e., $m_2 \neq m_2$, the one that remains unchanged is the true solution. The duality problem is solved.

Otherwise, i.e., both $m_1 = m_1$, and $m_2 = m_2$, the problem becomes *ill-conditioned*, and an additional image has to be acquired. The procedure returns to Step 3.

Ill-Conditioned Case:

It is important to analytically determine the ill-conditioned case, under which the z components of both \mathbf{n}_1 and \mathbf{n}_2 remain constant, namely $m_1 = m_1$ and $m_2 = m_2$. Rearranging Equations (11) (i.e., dividing (11-a) and (11-b) by (11-c), and moving k_1 and l_1 to the right), k_2 and l_2 are expressed in terms of k_1 and l_1 :

$$\begin{aligned} k_2 &= \frac{x_c}{z_c} (m_1 + m_2) - k_1 \\ l_2 &= \frac{y_c}{z_c} (m_1 + m_2) - l_1. \end{aligned} \quad (11)$$

Since \mathbf{n}_1 and \mathbf{n}_2 represent unit vectors,

$$\begin{aligned} k_1^2 + l_1^2 + m_1^2 &= 1 \\ k_2^2 + l_2^2 + m_2^2 &= 1. \end{aligned} \quad (12)$$

The substitution of Equation (11) into Equation (12) yields:

$$\left[\frac{x_c}{z_c} (m_1 + m_2) - k_1 \right]^2 + \left[\frac{y_c}{z_c} (m_1 + m_2) - l_1 \right]^2 + m_2^2 = 1. \quad (13)$$

Similarly, for Position 2 (in a general planar motion),

$$\left[\frac{x_c}{z_c} (m_1 + m_2) - k_1 \right]^2 + \left[\frac{y_c}{z_c} (m_1 + m_2) - l_1 \right]^2 + m_2^2 = 1. \quad (14)$$

Since we assumed that \mathbf{n}_1 was the true solution,

$$\begin{bmatrix} k_I \\ l_I \end{bmatrix} = \begin{bmatrix} \cos\theta & -\sin\theta \\ \sin\theta & \cos\theta \end{bmatrix} \begin{bmatrix} k_I \\ l_I \end{bmatrix}, \quad -\pi < \theta \leq \pi. \quad (15)$$

Substituting $m_1=m_1$ and $m_2=m_2$ and Equation (15) into (14), the following expression is obtained:

$$[x_c - \frac{z_c}{m_1 + m_2} (k_I \cos\theta - l_I \sin\theta)]^2 + [y_c - \frac{z_c}{m_1 + m_2} (k_I \sin\theta + l_I \cos\theta)]^2 + m_2^2 = 1. \quad (16)$$

Rearranging Equation (16) into a standard form for circular curves, we obtain,

$$\begin{aligned} [x_c - \frac{z_c}{m_1 + m_2} (k_I \cos\theta - l_I \sin\theta)]^2 + [y_c - \frac{z_c}{m_1 + m_2} (k_I \sin\theta + l_I \cos\theta)]^2 \\ = \frac{z_c^2}{(m_1 + m_2)^2} \cdot (1 - m_2^2). \end{aligned} \quad (17)$$

Equation (20) represents a group of circles, whose radius is

$$r_a = \frac{z_c}{m_1 + m_2} \sqrt{(1 - m_2^2)}, \quad (18)$$

and whose centers are located on another circle defined by

$$\begin{aligned} x &= \frac{z_c}{m_1 + m_2} (k_I \cos\theta - l_I \sin\theta), & -\pi < \theta \leq \pi. \\ y &= \frac{z_c}{m_1 + m_2} (k_I \sin\theta + l_I \cos\theta) \end{aligned} \quad (19)$$

Thus, if Equation (16) is satisfied by the motion at hand, an ill-conditioned problem results. The physical meaning of Equation (16) is that, if the center of a circular feature moves from an arbitrary Position 1: (x_c, y_c, z_c) to a new Position 2: (x_c, y_c, z_c) , there exist two singular θ values for the rotation of the surface normal. These correspond to the two solutions of the quadratic Equation (16).

It is worth noting that the singular θ angles are independent of the original position of the circular feature, whereas they depend on the original surface orientation \mathbf{n}_1 and the position of the second point B: (x_c, y_c, z_c) .

Experiments:

The experimental set-up described earlier in Section 3.1 was used here as well to verify the validity of the above technique. The object's translation was simulated by moving the camera parallel to the object's plane, where a rotation on this plane was achieved by turning the object manually to a desired angle utilizing an accurate set-up. The parameters m_1 and m_2 were estimated at two different positions. The normalized relative (scalar) differences, the z values of \mathbf{n}_1 and \mathbf{n}_2 , $\frac{m_1 - m_1}{m_1}$ and $\frac{m_2 - m_2}{m_2}$, were then calculated.

Figure 7 provides an example of a circular feature in planar motion. The position of the feature's center is pseudo-translated from Position 1: $[0, -50, 0]$ (mm) to Position 2: $[0, 0, 0]$ (mm). Relative changes in m_1 and m_2 were measured with respect to Position 1. We observe that the change in m_2 is significant, except in the $-10^\circ \sim 0^\circ$ range. Applying Equation (16), the singular value θ^* is calculated to be -5.0° . This θ^* value is in agreement with the experimental value noted in Figure 7.

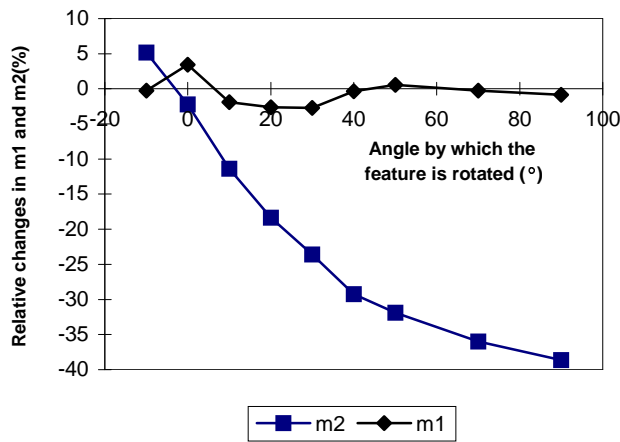


Figure 7. Changes in m_1 and m_2 in planar motion.

3.3 General Motion – Consideration of Additional Features

The orientation duality cannot be solved for a 3-D general motion without considering additional information. The reasoning behind the approach of using additional features is similar to those of the solution proposed in Section 3.1 and 3.2 for constrained motions, namely, to find a parameter which remains constant, for the true orientation, over consecutive images, while changing for the false one.

In the case of a constrained motion, we used the feature's normal vector itself, or simply its z component, as the invariant to distinguish the true solution from the false one. Similarly, here, for a “rigid-body” object in 3-D general motion, we use the fact that the relative distances among all the points on the object remain constant. However, we do not assume that these distances are known a priori.

3.3.1 A Co-planar Point

Consideration of an object point co-planar with the circular feature can lead to the solution of the orientation-duality problem. This co-planar point can, for example, be a corner point on the same object plane as the circular-feature and visible in the same image plane. Based on the rigid-body constraint, the distance between the point-feature and circular-feature's center, although unknown at the time of image acquisition and analysis, must remain constant in consecutive images. The concept is illustrated in Figure 8.

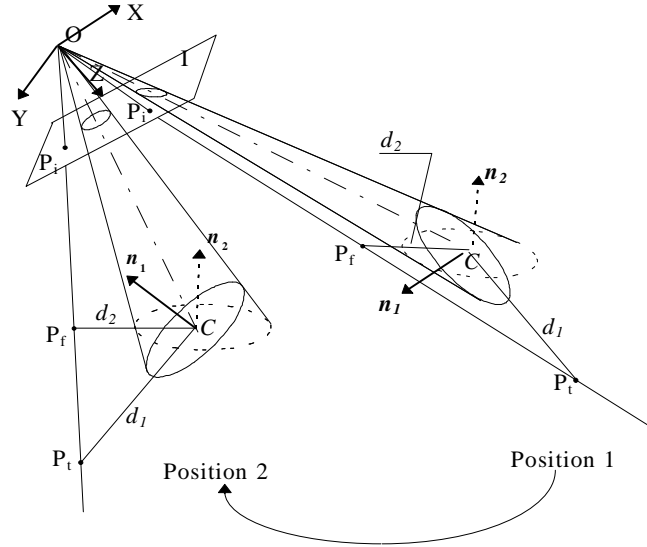


Figure 8. Solution for the duality problem: Considering a co-planar point.

Depicted in Figure 8 is a circular-feature moving from Position 1 to Position 2 in an arbitrary motion. Let P_t and P_t be the same “true” point-feature on the object at Position 1 and Position 2, respectively; and, let P_i and P_i be the corresponding points on the image plane I , defined by (x_i, y_i, f) and (x_i, y_i, f) , where f is the focal-length of the camera. Also, let Points P_f and P_f be the estimated false position of the point-feature in both images, resulting from the orientation-duality problem. In Figure 8, d_1 is the distance between the true point P_t and the circular-feature’s center C , and d_2 is the distance to the false point P_f . We define d_1 and d_2 in the same fashion for the second image.

Conjecture 3: Since all the points on a rigid body remain at constant distances with respect to one another, the distance between the point feature and circular-feature’s center at Position 1 should be equal to that at Position 2, i.e.,

$$d_1 = d_1, \quad (20)$$

while

$$d_2 \neq d_2. \quad (21)$$

It will be shown that, Conjecture 3, described by Equation (20) and Inequality (21), is always satisfied with a limited number of exceptions. For the solution of the duality problem using this conjecture, the distances d_1 , d_2 , d_1 and d_2 must be first calculated. Based on the constraint that the point under consideration is co-planar with the circular feature, the following equations can be established:

$$\mathbf{p}_t \cdot \mathbf{n}_1 = 0, \quad (22)$$

$$\mathbf{p}_f \cdot \mathbf{n}_2 = 0, \quad (23)$$

$$\mathbf{p}_t \cdot \mathbf{n}_1 = 0, \quad (24)$$

$$\mathbf{p}_f \cdot \mathbf{n}_2 = 0, \quad (25)$$

where \mathbf{p}_t , \mathbf{p}_f , \mathbf{p}_t and \mathbf{p}_f are defined as the “distance” vectors, with respect to the camera frame, pointing from C to points P_t , P_f , P_t and P_f , respectively.

Similarly, another set of vectors, \mathbf{r}_t , \mathbf{r}_f , \mathbf{r}_t and \mathbf{r}_f , can be defined as pointing from the camera’s origin, Point O, to P_t , P_f , P_t and P_f , respectively. Lying on the same lines of sight, OP_i and OP_i , these vectors can be related to the vectors, \mathbf{r}_i and \mathbf{r}_i , pointing from O to P_i and P_i , as follows:

$$\mathbf{r}_t = s_1 \mathbf{r}_i, \quad (26-a)$$

$$\mathbf{r}_f = s_2 \mathbf{r}_i, \quad (26-b)$$

$$\mathbf{r}_t = s_1 \mathbf{r}_i, \quad (26-c)$$

$$\mathbf{r}_f = s_2 \mathbf{r}_i, \quad (26-d)$$

where s_1 , s_2 , s_1 and s_2 are simply scaling factors. Since vectors \mathbf{r}_i and \mathbf{r}_i are determined by locating the coordinates of P_i and P_i in the image plane I, the positions for the point-feature, P_t and P_f , can be determined by solving for s_1 , s_2 , s_1 and s_2 .

Substituting Equations (26) into Equations (22) to (25), and expressing the vectors in terms of their components, we obtain:

$$\begin{cases} s_1 = \frac{k_1 x_c + l_1 y_c + m_1 z_c}{k_1 x_i + l_1 y_i + m_1 f}, \\ s_2 = \frac{k_2 x_c + l_2 y_c + m_2 z_c}{k_2 x_i + l_2 y_i + m_2 f} \end{cases}, \quad (27-a)$$

and

$$\begin{cases} s_1 = \frac{k_1 x_c + l_1 y_c + m_1 z_c}{k_1 x_i + l_1 y_i + m_1 f} \\ s_2 = \frac{k_2 x_c + l_2 y_c + m_2 z_c}{k_2 x_i + l_2 y_i + m_2 f} \end{cases} . \quad (27-b)$$

Therefore, the different positions of the point feature, in the camera frame, are expressed as follows:

$$\begin{cases} P_t = s_1(x_i, y_i, f) \\ P_f = s_2(x_i, y_i, f) \end{cases} , \quad (28-a)$$

and,

$$\begin{cases} P_t = s_1(x_i, y_i, f) \\ P_f = s_2(x_i, y_i, f) \end{cases} . \quad (28-b)$$

The distances between the point-feature and the circular-feature's center can now be calculated as,

$$\begin{aligned} d_1^2 &= (s_1 x_i - x_c)^2 + (s_1 y_i - y_c)^2 + (s_1 f - z_c)^2 \\ d_2^2 &= (s_2 x_i - x_c)^2 + (s_2 y_i - y_c)^2 + (s_2 f - z_c)^2 \end{aligned} , \quad (29-a)$$

and,

$$\begin{aligned} d_1^2 &= (s_1 x_i - x_c)^2 + (s_1 y_i - y_c)^2 + (s_1 f - z_c)^2 \\ d_2^2 &= (s_2 x_i - x_c)^2 + (s_2 y_i - y_c)^2 + (s_2 f - z_c)^2 \end{aligned} . \quad (29-b)$$

The procedure of solving the duality problem with one additional point-feature can be summarized as follows:

Step 1: Acquire the first image of the object and determine (i) the circular-feature's center (x_c, y_c, z_c) , (ii) the two possible orientations \mathbf{n}_1 and \mathbf{n}_2 , and (iii) the image coordinates of the additional point feature (x_b, y_b, f) .

Step 2: Solve for the two possible positions of the point-feature, P_t and P_f , using Equation (28-a).

Step 3: Apply Equation (29-a) to calculate the distances between the two possible point features and the circular-feature's center, namely d_1 and d_2 .

Step 4: Acquire a second image of the object and repeat Steps 1 through 3 to determine P_t and P_f using Equation (28-b), and d_1 and d_2 using Equation (29-b).

Step 5: Check whether $d_1=d_1$ and $d_2=d_2$; if true, then \mathbf{n}_1 , \mathbf{n}_2 must be the true orientations of the circular feature, while P_t and P_f are the true positions of the point feature. Thus, the duality problem is solved.

If, however, both $d_1=d_1$ and $d_2=d_2$, the duality problem is *ill-conditioned*, and a third image is necessary.

Ill-Conditioned Case:

In order to determine analytically when the ill-conditioned case occurs, the problem is formulated here as follows: Given a rigid-body object, with a circular feature and a point feature on one of its surfaces, moving from Position 1 to Position 2, what values of \mathbf{n}_1 and \mathbf{n}_2 , will result in an ill-conditioned problem, i.e., for which $d_1=d_1$ and $d_2=d_2$?

In mathematical terms, the above implies solving for s_1 and s_2 in the following, which are obtained by equating (29-a) and (29-b),

$$d_1^2 = (s_1 x_i - x_c)^2 + (s_1 y_i - y_c)^2 + (s_1 f - z_c)^2 = d_1^2, \quad (30-a)$$

and

$$d_2^2 = (s_2 x_i - x_c)^2 + (s_2 y_i - y_c)^2 + (s_2 f - z_c)^2 = d_2^2. \quad (30-b)$$

Since the only unknown in Equation (30-a) is s_1 , and the only unknown in Equation (30-b) is s_2 , we can solve for s_1 and s_2 individually. As scaling factors, s_1 and s_2 must have real values. Since \mathbf{n}_1 and \mathbf{n}_1 are assumed to be the true orientations for the circular feature, there must exist real roots for Equation (30-a). For Equation (30-b), however, real solutions for s_2 might not exist. Therefore, the ill-conditioned problem can only occur when there is a real solution for s_2 in Equation (30-b).

Once the values of s_1 and s_2 (assuming s_2 has a real solution) are obtained, we can solve for \mathbf{n}_1 and \mathbf{n}_2 that satisfy the ill-conditioned problem. Rearranging Equations (27a and 27b), by moving the denominator of the right-hand-side to the left and moving all the terms to the left, we obtain:

$$k_1(x_c - s_1 x_i) + l_1(y_c - s_1 y_i) + m_1(z_c - s_1 f) = 0, \quad (31-a)$$

and

$$k_2(x_c - s_2 x_i) + l_2(y_c - s_2 y_i) + m_2(z_c - s_2 f) = 0. \quad (31-b)$$

In the above equations, there are six unknowns, three for \mathbf{n}_1 (k_1 , l_1 , m_1) and three for \mathbf{n}_2 (k_2 , l_2 , m_2).

Based on the symmetry of the two orientations for the circular-feature, we can obtain four more equations:

$$k_1 + k_2 = (m_1 + m_2) \frac{x_c}{z_c}, \quad (31-c)$$

$$l_1 + l_2 = (m_1 + m_2) \frac{y_c}{z_c}, \quad (31-d)$$

$$k_1^2 + l_1^2 + m_1^2 = 1, \quad (31-e)$$

$$\text{and} \quad k_2^2 + l_2^2 + m_2^2 = 1. \quad (31-f)$$

Combining (31-a) through (31-f), we have six equations and six unknowns. The first four equations are linear, while the last two are quadratic. By Bezout's theorem [7], since all Equations (31) are independent, there exist $1^4 \cdot 2^2 = 4$ solutions. As (k_1, l_1, m_1) and (k_2, l_2, m_2) are feature orientations, only real solutions are acceptable. The number of acceptable orientations should therefore be less than four. In other words, when the object moves from Position 1 to Position 2 in a general motion, there would not be more than four possible orientations of the object that would result in an ill-conditioned problem for the detection of the true orientation of the circular-feature.

Experiments:

The technique described above was verified by experiments using an object with a circular feature and an artificial co-planar point feature. The object motion was simulated by moving the camera on a virtual sphere's surface, with the camera always pointing toward the circular feature's center to maximize visibility, Figure 9, [Xiaoyu paper].

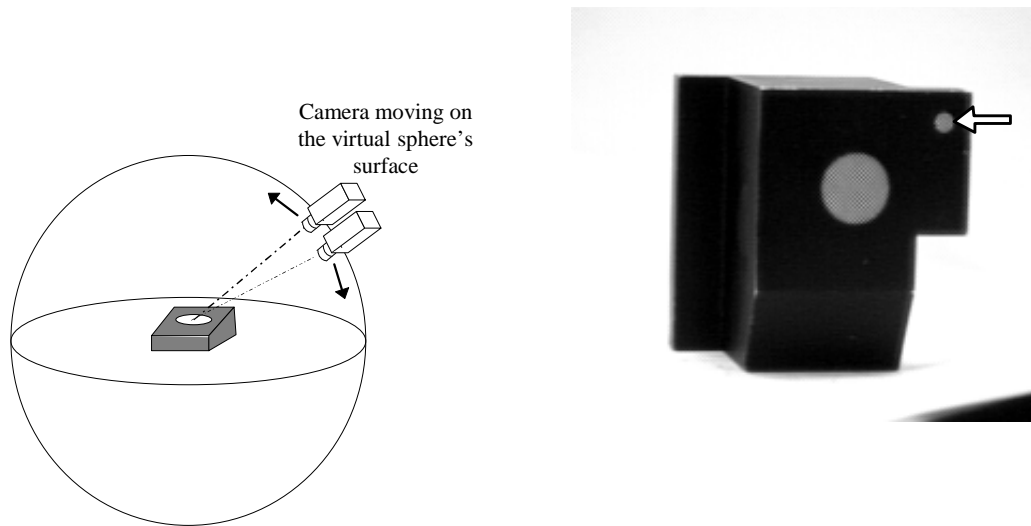


Figure 9. (a) 3-D camera movement; and, (b) Artificial features.

Following Steps 1 through 4 stated above, the relative changes in the parameters d_1 and d_2 , i.e., $\frac{d_1 - d_1}{d_1}$ and $\frac{d_2 - d_2}{d_2}$, were calculated and plotted in Figure 10, for 10° -incremented camera movements. As can be noted, d_1 remains almost constant, while change in d_2 varies significantly. Thus, d_1 is clearly the true solution.

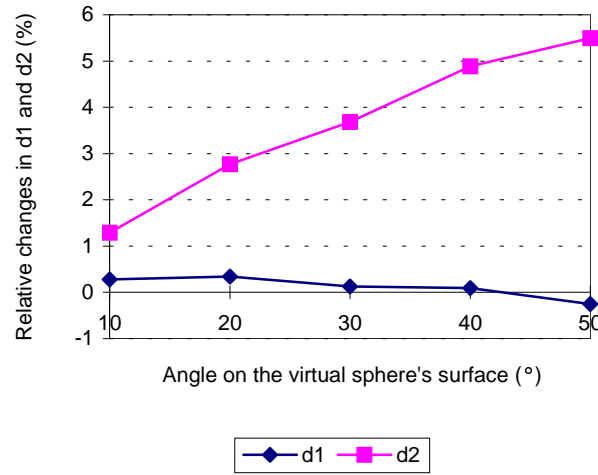


Figure 10. Changes in the distance d_1 and d_2 , when the camera is moved on the sphere's surface.

In another example, the camera was moved along the radius of the sphere toward the object, [Tony Thesis]. As in the case of motion over the sphere's surface, d_2 changed while d_1 remained relatively constant. It was noted that, the rate of change in d_2 was higher at closer camera distances to the object. Thus, one must operate in optimal distance range in order to determine the true feature orientation with high confidence.

3.3.2 A Co-planar Line

Since the object in motion is assumed to be a rigid body, the distance between a co-planar line feature and the circular-feature's center can be used as an invariant to solve the duality problem, even though its value is not known a priori. In this section, we assume that a co-planar linear edge has already been extracted from the image using

common edge detectors, and that its mathematical form has also been determined. Figure 11. depicts an object motion from Position 1 to Position 2. l_1 and l_1 are the line-features on the object in Position 1 and 2, respectively, while l_2 and l_2 are the corresponding possible lines due to the orientation duality. l_i and l_i are the projections of the same lines in the image Plane I in the two consecutive images.

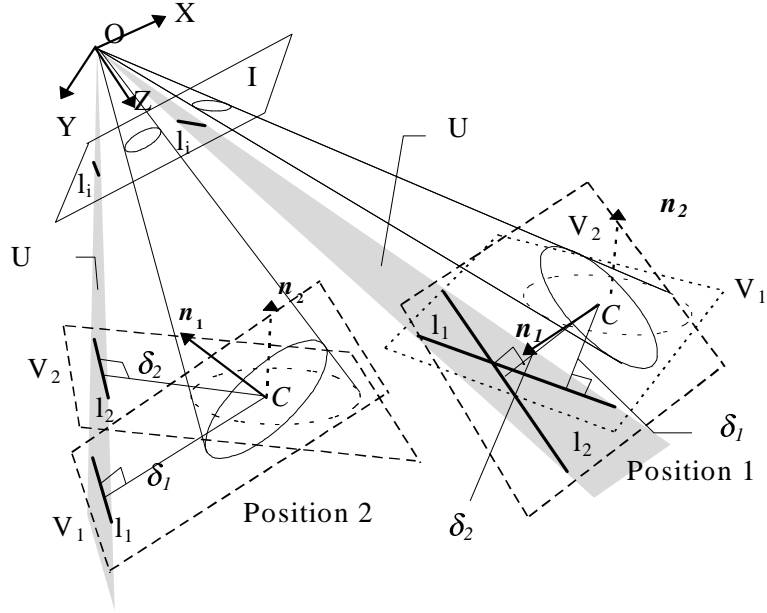


Figure 11. Solution for the duality problem with an additional line-feature.

The parameter δ_l is defined as the shortest distance between the line-feature l_1 and the circular-feature's center C. Similarly, δ_2 , δ_l and δ_2 represent corresponding distances between the line-feature and the circular-feature's center.

Conjecture 4: Since the object is assumed to be a rigid body, i.e., the distances among all the points on the object surface remain constant during object motion,

$$\delta_l = \delta_l, \quad (32)$$

if one assumes that l_1 is the true position of the line feature. On the other hand, it will be shown that, with a limited number of exceptions,

$$\delta_2 \neq \delta_2. \quad (33)$$

To use Conjecture 4, defined by Equation (32) and Inequality (33), δ_1 , δ_2 , δ_l and δ_2 have to be calculated first. Knowing the camera's focal length, f , the image plane I can be defined at $z=f$ with respect to the camera frame, Figure 11. The projection of the line-feature l_i within the plane I can be defined by:

$$ax + by + c = 0 . \quad (34)$$

Let us define the plane that passes through both the focal point O and Line l_i as Plane U, and the planes on which the circular feature possibly lies as Planes V_1 and V_2 . Since the line-feature must lie in Plane U, also given that the line and the circular-feature are co-planar, we can solve for the line positions by intersecting Plane U with Planes V_1 and V_2 .

First, we obtain the equation for Plane U as:

$$ax + by + \frac{c}{f}z = 0 . \quad (35)$$

To simplify the last coefficient of the equation, let $f=1$. Equation (35), with a modified constant, c , is then reduced to,

$$ax + by + cz = 0 . \quad (36)$$

Similarly, at Position 2, for Line l_i :

$$a x + b y + c = 0 , \quad (37)$$

and for Plane U :

$$a x + b y + c z = 0 . \quad (38)$$

The orientations of Planes V_1 and V_2 are defined by unit surface normals, \mathbf{n}_1 and \mathbf{n}_2 . Plane V_1 can then be expressed by:

$$k_1(x - x_c) + l_1(y - y_c) + m_1(z - z_c) = 0 , \quad (39)$$

where (k_I, l_I, m_I) are the components of \mathbf{n}_I , and (x_c, y_c, z_c) are the coordinates of the circular-feature's center. After collecting all the constant terms, Equation (39) is reduced to,

$$k_I x + l_I y + m_I z + w_I = 0, \quad (40)$$

where parameter w_I is defined by,

$$w_I = -k_I x_c - l_I y_c - m_I z_c. \quad (41)$$

Similarly, for Plane V_2 , we have,

$$k_2 x + l_2 y + m_2 z + w_2 = 0, \quad (42)$$

where parameter w_2 is defined by,

$$w_2 = -k_2 x_c - l_2 y_c - m_2 z_c. \quad (43)$$

The intersection of Plane U and Plane V_1 yields Line l_1 in the following form:

$$\frac{N_I x - b w_I}{L_I} = \frac{N_I y + w_I a}{M_I} = z, \quad (44)$$

$$L_I = \begin{vmatrix} b & c \\ l_I & m_I \end{vmatrix}$$

$$\text{where, } M_I = \begin{vmatrix} c & a \\ m_I & k_I \end{vmatrix}.$$

$$N_I = \begin{vmatrix} a & b \\ k_I & l_I \end{vmatrix}$$

Similarly, the equation for Line l_2 is obtained as,

$$\frac{N_2 x - b w_2}{L_2} = \frac{N_2 y + w_2 a}{M_2} = z, \quad (45)$$

$$L_2 = \begin{vmatrix} b & c \\ l_2 & m_2 \end{vmatrix}$$

$$\text{where, } M_2 = \begin{vmatrix} c & a \\ m_2 & k_2 \end{vmatrix}.$$

$$N_2 = \begin{vmatrix} a & b \\ k_2 & l_2 \end{vmatrix}$$

For Position 2, l_1 and l_2 can be acquired in the same fashion. Once the line equations are determined, the distances δ_1 , δ_2 , δ_1 and δ_2 can be calculated [7]. For Position 1, and \mathbf{n}_1 , we have

$$\delta_1^2 = \frac{1}{L_1^2 + M_1^2 + N_1^2} \left[(y_c N_1 - z_c M_1 + aw_1)^2 + (z_c L_1 - x_c N_1 + bw_1)^2 + (x_c M_1 - y_c L_1 + cw_1)^2 \right]. \quad (46)$$

δ_2 , δ_1 and δ_2 can be calculated similarly. Using Equation (32) and Inequality (33), we can determine the true surface orientation.

The procedure of solving the duality problem with one additional co-planar line-feature can be therefore summarized as follows:

Step 1: Acquire the first image of the object, extract a line-feature and represent it in the form of Equation (34). Calculate (i) the circular-feature's center (x_c, y_c, z_c) , and (ii) the two possible orientations, \mathbf{n}_1 and \mathbf{n}_2 , for the same circular-feature. The parameters a, b, c, w_1 and w_2 are subsequently determined.

Step 2: Solve for the possible 3-D position of the line-features, using Equations (44) and (45). The parameters L_1, M_1, N_1, L_2, M_2 and N_2 are then calculated.

Step 3: Apply Equation (46) to calculate the distances between the line-feature and circular-feature's center, δ_1 and δ_2 .

Step 4: Acquire a second image of the object. Follow the same steps as for the first image, to solve for l_1, l_2, δ_1 and δ_2 , (Steps 1 through 3).

Step 5: Compare δ_1 and δ_2 with δ_1 and δ_2 , if both Equation (32) and Inequality (33) are satisfied, \mathbf{n}_1 and \mathbf{n}_1 would be the true orientations of the circular feature. Also, \mathbf{l}_1 and \mathbf{l}_1 would be the true positions of the line feature. Thus, the duality problem is solved.

If, however, Inequality (33) is not satisfied, i.e.,

$$\delta_1 = \delta_2, \quad (47)$$

the duality problem cannot be solved. This situation is an *ill-conditioned problem*. Similar to the previous cases, a third image is needed to solve the duality ill-conditioned problem.

Ill-Conditioned Case:

When the object is first moved to Position 1, the values of δ_1 and δ_2 are determined. For the problem to become ill-conditioned, δ_1 and δ_2 , at Position 2, have to be equal to δ_1 and δ_2 , respectively. Therefore, the following equations, obtained by combining Equations (32), (33), (46) and (47), must be satisfied:

$$\begin{aligned} \delta_1^2 &= \delta_2^2 \\ &= \frac{1}{L_1^2 + M_1^2 + N_1^2} [(y_c N_1 - z_c M_1 + a w_1)^2 + (z_c L_1 - x_c N_1 + b w_1)^2 + (x_c M_1 - y_c L_1 + c w_1)^2] \end{aligned} \quad (48-a)$$

and

$$\begin{aligned} \delta_2^2 &= \delta_1^2 \\ &= \frac{1}{L_2^2 + M_2^2 + N_2^2} [(y_c N_2 - z_c M_2 + a w_2)^2 + (z_c L_2 - x_c N_2 + b w_2)^2 + (x_c M_2 - y_c L_2 + c w_2)^2] \end{aligned} \quad (48-b)$$

Based on the relationships in Equation (44) and (45), there exist three unknowns (k_1 , l_1 and m_1) in Equation (48-a), and three unknowns (k_2 , l_2 and m_2) in Equation (48-b). Due to the symmetry condition of \mathbf{n}_1 and \mathbf{n}_2 :

$$k_1 + k_2 = (m_1 + m_2) \frac{x_c}{z_c}, \quad (48-c)$$

$$l_1 + l_2 = (m_1 + m_2) \frac{y_c}{z_c}, \quad (48-d)$$

and, since \mathbf{n}_1 and \mathbf{n}_2 are unit vectors,

$$k_1^2 + l_1^2 + m_1^2 = 1 \quad (48-e)$$

$$k_2^2 + l_2^2 + m_2^2 = 1. \quad (48-f)$$

The set of Equations (48) comprises six equations for six unknowns. The roots of this set of equations, (k_1 , l_1 , m_1) and (k_2 , l_2 , m_2), are the singular orientations of the circular feature that result in the ill-conditioned problem. Based on Bézout's Theorem [7], since each equality in (48) is independent of one another, there exist $2^4 \cdot 1^2 = 16$ solutions. (k_1 , l_1 , m_1) and (k_2 , l_2 , m_2) being orientations of the circular feature, only real solutions are allowed. Therefore, there should be no more than 16 possible orientations that will result in an ill-conditioned problem for the detection of the true orientation of the features.

Experiments:

The technique described above was verified by experiments using an object with co-planar artificial circular and linear features, Figure 13. The camera was moved in the same fashion as depicted in Figure 9. Figure 13. is a plot of relative changes in δ_1 and δ_2 at different test positions when the camera was moved on the sphere's surface at 10° increments. As can be noted, δ_1 remains relatively constant, while δ_2 changes significantly as the object moves away from the initial position.

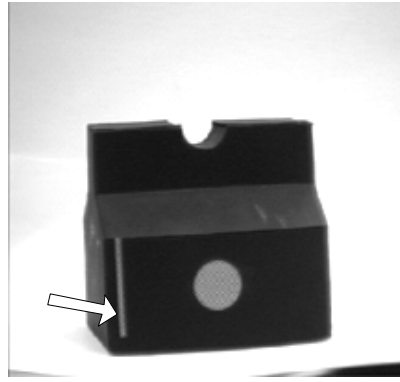


Figure 12. Artificial features.

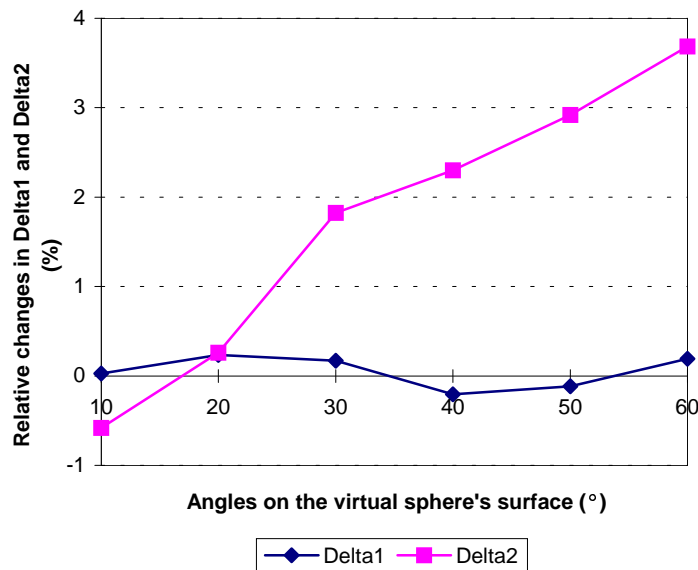


Figure 13. Changes in δ_1 and δ_2 , when the camera is moving on a virtual sphere's surface.

4. Discussion and Conclusions

Circular features can be very useful in object-motion estimation. However, their orientation-duality problem must be solved first. The first solution presented in this paper is applicable to constrained motions: motion along 3-D straight lines or general planar motion. Experiments showed that the methods are in general effective in practice.

The second solution approach for 3-D general motion advocates the use of additional features. Based on the assumption that the object is a rigid body, the distances from the circular feature to additional features, though unknown a priori, are used as invariants to solve the duality problem. Experiments also showed that the methods are effective in practice. Ill-conditioned positions do exist, however they can be found by solving a set of linear and quadratic equations.

In conclusion, for all the methods proposed in this paper, two consecutive images are sufficient to obtain uniquely the circular feature's 3-D pose estimation.

References

- [1] Magee, M.J. and Aggarwal, J.K., "Determine the position of a robot using a single calibration object", *International Conference on Robotics and Automation*, Atlanta, GA, Mar. 1984, pp. 140-149.
- [2] Ussain, B. and Kabuka, M.R., "Real-time system for accurate three-dimensional position determination and verification", *IEEE Transactions on Robotics and Automation*, Vol. 6, No. 1, Feb. 1990, pp. 31-43.
- [3] Fainman, Y., Feng, L. and Koren, Y., "Estimation of absolute spatial position of mobile systems by hybrid opto-electronic processor", International Conference on Systems, Man and Cybernetics, Cambridge, MA, Nov. 1989, pp. 651-657.
- [4] Shin, Y.C. and Ahmad, S., "3D Location of circular spherical features by monocular model-based vision", in IEEE International Conference on Systems, Man and Cybernetics, Boston, MA, Nov. 1989, pp. 576-581.
- [5] R. Safaee-Rad, K.C. Smith, B. Benhabib, and I. Tchoukanov., "3-D-Location Estimation of Circular Features for Machine Vision", *IEEE Transactions on Robotics and Automation*, Vol. 8, No. 5, 1992, pp. 624-640.

[6] Ma, S.D., “Conics-Based Stereo, Motion Estimation, and Pose Determination”, *International Journal of Computer Vision*, Vol. 10, No. 1, 1993, pp. 7-25.

[7] Coolidge, J.L., *A Treatise on Algebraic Plane Curves*, Dover Publication, 1959.

[8] Horn, B.K.P, *Robot Vision*, The MIT press, McGraw-Hill Book Company, 1986.

[9] Pavlidis, T., “A Critiacl Survey of Image Analysis Methods”, *Proc., International Conference on Pattern Recognition*, pp. 502-511, 1986.

[10] Nitzan, D., “Three-Dimensional Vision Structure for Robot Applications”, *IEEE Transactions on Pattern Recognition and Machine Intelligence*, Vol. 10, no.3, pp. 291-309, May 1988.

[11] Chin, R.T. and Dyer, C.D., “Model-Based Recognition in Robot Vision”, *Computing Surveys*, Vol. 18, No.1, pp. 67-108, March, 1986.

[12] Safaee-Rad, R., *An Active-Vision System for 3D-Object Recognition in Robotic Assembly Workcells*, Ph.D. Dissertation, University of Toronto, 1991.

[13] Srinivasan, M.V., Lehrer, M., Zhang, S.W. and Horridge G.A., “How honeybees measure their distance from objects of unknown size”, *Journal of Comparative Physiology A*, Vol. 165, 1989, pp.605-613.

[14] G.L. Foresti, V. Murino, “Moving-Object Recognition from an Image Sequence for Autonomous Vehicle Driving”, *Time-Varying Image Processing and Moving Object Recognition*, 3, – V. Cappelini (Ed.) Elsevier Science, 1994, pp. 383-390.

[15] J.K. Aggarwal and N. Nandhakumar, “On the Computation of Motion from Sequence of Images: A Review”, *Proceedings of the IEEE*, Vol. 76, No. 8, August 1988, pp. 971-935.

[16] M. Yamamoto, “Pose from Motion: A Direct Method”, *Time-Varying Image Processing and Moving Object Recognition*, 3, –V. Cappelini (Ed.) Elsevier Science, 1994, pp. 287-294.

[17] Aloimonos, Y., *Active Perception*, Lawrence Erlbaum, 1993.

[18] J.T. Feddema and C.S.G. Lee, “Adaptive Image Feature Prediction and Control for Visual Tracking with a Hand-Eye Coordinated Camera”, *IEEE Transactions on Systems, Man and Cybernetics*, Vol. 20, No. 5, September/October 1990, pp. 1172-1183.

[19] J. Hwang, Y. Ooi, and S. Ozawa, “An Adaptive Sensing System with Tracking and Zooming a Moving Object”, *IEICE Transactions on Information & Systems*, Vol. E76-D, No. 8, Aug. 1993. pp. 926-934.

[20] D. Murray and A. Basu, “Active Tracking”, *Proceedings of the 1993 IEEE International Conference on Intelligent Robots and Systems*, Yokohama, Japan, July, 1993, pp. 1021-1028.

[21] Shmuel, A., and Werman, M., “Active Vision: 3D from an image sequence”, *IEEE International Conference on Pattern Recognition*, Atlantic City, New Jersey, Vol. I, pp.48-54, June 1990.

[22] Stoll, H.W., “Automation: Teacher and Test for Good Product Design”, Lane, J.D., *Automated Assembly*, Society of Manufacturing Engineers, Dearborn, MI, 1986, pp. 117-129.

[23] Eversheim, W. and Muller W., “Assembly Orientated Design”, Programmable Assembly: International Trends in Manufacturing Technology, pp.143-153, IFS publication, UK, 1984.

[24] M. Yamamoto and K. Ikeda, “Stereoscopic Correcting Pose of 3D Model of Object”, *Time-Varying Image Processing and Moving Object Recognition*, 3, –V. Cappelini (Ed.) Elsevier Science, 1994, pp. 127-134.

[25] T.S. Huang and A.N. Netravali, “Motion and Structure from Feature Correspondence: A Review”, *Proceedings of the IEEE*, Vol. 82, No. 2, Feb. 1994, pp. 252-268.

[26] Liu, Y.C. and Huang, T.S., “Estimation of Rigid Body Motion Using Straight Line Correspondences”, *IEEE workshop on Motion*, Kiawah Island, SC, may 7-9, 1986, pp. 47-52.

[27] Spetsakis, M.E. and Aloimonos, J., “Close form solutions to the structure from motion problem from line correspondence”, *Proceedings of AAAI*, Seatle, WA, July 1987, pp.738-743.

[28] Aggarwal, J.K. and Wang, Y.F., “Analysis of a sequence of images using point and line correspondence”, *International Conference on Robotics and Automation*, Raleigh, NC, Mar. 1987.

[29] Ma, S.D., “Conics-Based Stereo, Motion Estimation, and Pose Determination”, *International Journal of Computer Vision*, Vol. 10, No. 1, 1993, pp. 7-25.

[30] McVey, E.S. and Jarvis, G.L., “Ranking of Patterns for Use in Automation”, *IEEE Transactions on Industrial Electronics and Control Instrumentation*, Vol.24 (2), pp. 211-213, 1977.

[31] Kunii, T.L., editor, *Three-Dimensioanl Object Recognition from Range Images*, Springer-Verlag publication, 1992.

[32] Besl, P.J. and Jain, R.C., “Invariant surface characteristics for 3-D object recognition in range image”, *Computer Vision, Graphics and Image Processing*, Vol. 33, 1986, pp. 30-80.

[33] Brady, M. and Ponce, J. “Toward a surface primal sketch”, *Proc. IEEE Conference on Computer Vision and Pattern Recognition*, 1985, pp.420-425.

[34] Fan, T.J., Medioni, G. and Nevatia, R. “Segmented descriptions of 3-D surfaces. *IEEE Journal on Robotics and Automation*, RA-3, 1987, Vol. 3, No. 6, pp. 527-538.

[35] Vemuri, B.C. and Aggarwal, J.K., “Representation and recognition of objects from dense range maps”. *IEEE Transactions on Circuits and Systems*, 1987, Vol. CAS-34, No. 11, pp. 1351-1363.

[36] Chien, C.H. and Aggarwal, J.K., “Generation of Volume/Surface octree from range data. Proc. *IEEE Conference on Computer Vision and Pattern Recognition*, 1988, pp.254-260.

[37] Osgood, W.F. and Granstein, W.C., *Plane and Solid Analytical Geometry*, 1921

[38] Coolidge, J.L., *A Treatise on Algebraic Plane Curves*, Dover Publication, 1959.

[10] R. Safaee-Rad, I. Tchoukanov, X. He, K.C. Smith, and B. Benhabib, “An Active-Vision System for Recognition of Pre-Marked Objects in Robotic Assembly Workcells”, *IEEE Conference on Computer Vision and Pattern Recognition*, N.Y. City, U.S.A., June 1993, pp. 722-723.

[11] R. Safaee-Rad, K.C. Smith, B. Benhabib and I. Tchoukanov, “Application of Moment and Fourier Descriptors to the Accurate Estimation of Elliptical Shape Parameters”, *Pattern Recognition Letters*, Vol. 13, July 1992, pp. 479-508.

[12] E. Mosnat, *Problemes de Geometrie Analytique*, Vol. III, Third Edition, Paris Vuibert, 1944.

[13] Bell, R.J.T., An Elementary Treatise on Coordinated Geometry of the Three Dimensions, Macmillan & Co. Ltd, London, First Edition, 1910, Third Edition, 1944.

[14] R. Safaee-Rad, K.C. Smith, B. Benhabib, and I. Tchoukanov., “3D-Location Estimation of Circular Features for Machine Vision”, *IEEE Transactions on Robotics and Automation*, Vol. 8, No. 5, 1992, pp. 624-640.

[15] I. Tchoukanov, R. Safaee-Rad, K.C. Smith, and B. Benhabib, “The Angle-of-Sight Signature for 2D-Shape Analysis of Manufactured Objects”, *Journal of Pattern Recognition*, Vol. 25, No. 11, Dec. 1992, pp. 1289-1305.

[16] J.T. Feddema, and C.S.G. Lee, “Adaptive Image Feature Prediction and Control for Visual Tracking with a Hand-Eye Coordinated Camera”, *IEEE Transactions on Systems, Man, and Cybernetics*, Vol. 20, No. 4, 1990, pp. 1172-1183.

[17] G.T. Uber, “Illumination and Imaging of Moving Objects”, *SPIE Optics, Illumination, and Image Sensing for Machine Vision III*, 1988, Vol. 1005, pp. 2-5.

[18] D. Hujic, G. Zak, E. Croft, R.G. Fenton, J.K. Mills and Benhabib, “An Active Prediction, Planning and Execution System for Interception of Moving Objects”, *IEEE International Symposium on Assembly and Task Planning*, Pittsburgh, Aug. 1995, In Print.